Effect of Substrate Texture on Electroplating

A REPORT SUBMITTED IN PARTIAL FULFILMENT
OF THE REQUIREMENT FOR THE DEGREE OF

Bachelor of Technology
in
Metallurgical and Materials Engineering

By

KRISHNAM SINGH CHAUHAN

SANJEEB KUMAR LAKRA

DEPARTMENT OF METALLURGICAL AND MATERIALS ENGINEERING
NATIONAL INSTITUTE OF TECHNOLOGY
ROURKELA

Effect of Substrate Texture on Electroplating

A REPORT SUBMITTED IN PARTIAL FULFILMENT
OF THE REQUIREMENT FOR THE DEGREE OF

Bachelor of Technology
in
Metallurgical and Materials Engineering

By

KRISHNAM SINGH CHAUHAN
(Roll No. 10604043)

SANJEEB KUMAR LAKRA
(Roll No. 10604007)

Under the guidance of

Prof. A. Basu

DEPARTMENT OF METALLURGICAL AND MATERIALS ENGINEERING
NATIONAL INSTITUTE OF TECHNOLOGY, ROURKELA

National Institute of Technology
Rourkela

CERTIFICATE

This is to certify that the thesis entitled, "**EFFECT OF SUBSTRATE TEXTURE ON ELECTROPLATING**" submitted by **Mr. KRISHNAM SINGH CHAUHAN** in partial fulfillment of the requirements for the award of Bachelor of Technology Degree in Metallurgical and Materials Engineering at the National Institute of Technology, Rourkela (Deemed University) is an authentic work carried out by him under my supervision and guidance.

To the best of my knowledge, the matter embodied in the thesis has not been submitted to any other University / Institute for the any Degree or Diploma.

DATE:

Prof. A. Basu
Dept. of Metallurgical and Materials Engineering
National Institute of Technology, Rourkela-769008

ACKNOWLEDGEMENT

With great pleasure, I would like to express my deep sense of gratitude to my guide **Dr. A. Basu**, Metallurgical & Materials Engineering Department, for his valuable guidance, constant encouragement and kind help at different stages for the execution of this dissertation work.

I would also like to thank **Tata Steel, Jamshedpur** for providing the textured steel samples and various experimental data.

I am sincerely grateful to, **Dr. B.B. Verma**, Head of the Department, Metallurgical & Materials Engineering, for providing valuable departmental facilities.

I would like to extend my sincere thanks to our project coordinators **Prof.A.K.Panda** and **Prof. M.Kumar** for helping us at each and every step in bringing out this report.

I would also like to thank **Mr. Samir Pradhan, Mr. Rajesh Pattnaik** and **Mr. Hembrem** for helping me out during different phases of experimentation.

Last but not the least; I would also like to thank all my friends for their help and co-operation and especially to **Sanjeeb Lakra** for helping me throughout the project work.

N.I.T. ROURKELA
DATE:

KRISHNAM SINGH CHAUHAN
B.Tech (100604043)
Dept. of Metallurgical and Materials Engineering

Contents

List of Figures: **Page No.**

List of Tables: **Page No.**

1. Introduction

Electroplating studies have been conducted extensively in the past due to their lower cost and fastness. Mechanical and functional properties of such coatings depend highly on the chemistry and the structure of the same. Deviation from random orientation in the crystallographic directions is known as preferred orientation or texturing in materials. Depending upon the texture, material property may be highly anisotropic. So, texture study of coating is of prime importance and moreover how the texturing phenomenon is occurring in coatings is also to be examined. The influence of substrate texture and electroplating conditions on the texture and surface morphology of electrodeposits is still unclear. Preferred orientation or texturing is governed by the lowest energy condition. During growth of a specific phase, there is a competition between strain energy and surface energy. But, experimental analysis of such system has not been done widely. In this study, an attempt has been made to study the role of substrate texture on the coating texture. Routine microscopic study and surface mechanical testing was also carried out.

2. Literature Review

2.1 INTRODUCTION

From the moment any material is released from the point of production, it is subjected to some form of materials degradation although such degradation may not be readily observed or measured. The rapid rusting of freshly machined steel surfaces is a common example of immediate materials degradation.

Such damage continues throughout the lifetime and materials degradation of any component be a limiting factor. No known service environment provides perfect immunity from materials degradation. Under atmospheric conditions, electrochemical corrosion is the most significant degradation process in economic terms. In outer space, although the absence of atmosphere precludes corrosion, radiation damage can be severe. Corrosion, radiation damage and many other mechanisms all have a shared feature of reducing the performance of engineering materials to cause premature failure of components and devices. A simple definition of materials degradation is that it is the consequence of a wide range of physical processes; it is almost universal in occurrence and is a major engineering problem.

The term surface engineering was coined for the first time in England in the 70s. Surface engineering refers to control of problems originating from the surface of engineering components. It is generally considered that the surface of a component is much more vulnerable to damage than the interior of the component and that surface originated damage will eventually destroy the component. Most types of materials degradation such as, wear, corrosion and fracture are usually located at the surface of a component. As a result of this concentration of damage processes at the surface of a component, surface engineering is essential to control these damage processes.

2.2 MATERIALS DEGRADATION

Materials degradation can be defined in terms of loss of performance of an engineering system. Loss of performance can relate to many parameters, e.g. loss of reflectivity in optical equipment caused by fungal attack. A more common example might be the loss in mechanical strength of a structural component exposed to a corrosive medium. For any item of equipment, there is a critical minimum level of performance, e.g. whether a useful image is

obtained from the optical system or whether the mechanical structure will collapse due to corrosion damage. For the engine with worn cylinders, wear can increase the clearance between piston ring and cylinder to such an extent that there is no compression of combustion gases. In this case the engine can be considered to have failed, as it will no longer be able to pull the car or truck up the hill. A mechanical degradation proceeds at a rate that varies with local conditions and failure occurs if the performance declines to below the critical level. Loss of efficiency occurs if performance declines but remains above the critical level during the service lifetime.

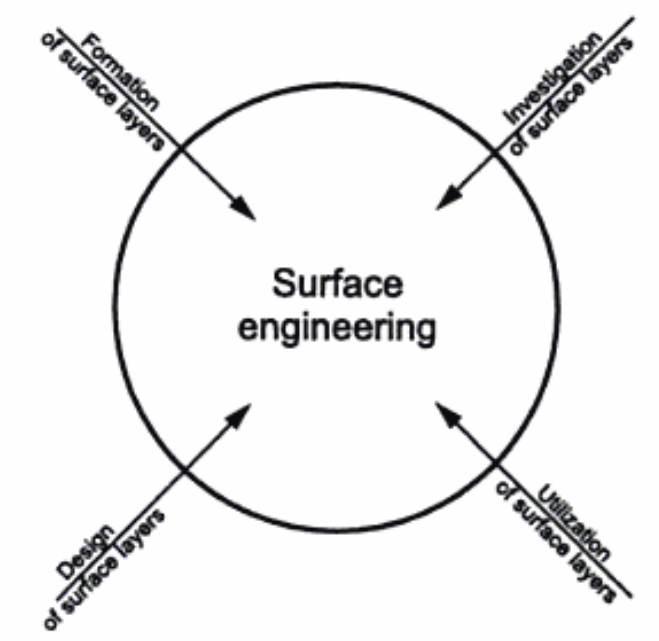

Fig. 2.1 Area of activity of Surface Engineering

Referring to the previous examples of the optical system and mechanical structure, loss of efficiency could involve a progressive distortion of the image for the optical system and load restrictions for the mechanical structure. Some loss of performance is inevitable unless very expensive control measures are implemented, e.g. constructing a car from stainless steel instead of plain steel. The scientific study of degradation of engineering materials can be summarized as predicting the rate of decline of performance. Engineering analysis of materials degradation is directed at finding the factors controlling this gradient and how to reduce it.

There are three basic categories of materials degradation, physical, chemical or biological in origin. Physical origin refers to the effect of force, heat and radiation. Chemical origin relates to destructive reactions between the material and chemicals that contact it. Biological origin includes all interactions between life forms and engineering materials.

Materials degradation such as thermal damage or chemical reactions, which are either entirely physical or chemical in nature, coexists with combined forms of materials degradation such as corrosive-wear. Materials degradation is an uncontrolled process without restriction on interactions between seemingly unrelated events. Environmental conditions also exert a strong effect on materials degradation with the result that any given materials degradation problem is effectively dependent on locality. As will be shown in later chapters, there is a wide range of possible interactions or synergy between degradation processes and considerable care is needed to predict which of these interactions are significant to any given situation. [1]

2.3 SURFACE ENGINEERING

Surface engineering is a comparatively recent term that refers to control of problems originating from the surface of engineering components. The objective of surface engineering is to ensure that performance remains far above the critical level for the entire service lifetime of a system. It is generally considered that the surface of a component is much more vulnerable to damage than the interior of the component and that surface originated damage will eventually destroy the component. Most types of materials degradation such as, wear, corrosion and fracture are usually located at the surface of a component. As a result of this concentration of damage processes at the surface of a component, surface engineering is essential to control these damage processes.

A time-honored solution to the problem of materials degradation is to try and shield the material from the hostile agent. For example, painting is a well-established example of this practice and serves to shield a metal (or wood) from water and oxygen. The range of techniques available to prevent materials degradation by shielding has expanded enormously in recent years.

Shielding is usually achieved by coating the material with another substance or by generating a surface modified layer, which is more durable than the original material. Another form of shielding is to inhibit the chemical processes that directly control degradation. Cathodic protection where an electrical potential is used to suppress electrochemical corrosion of metals is an example of this latter method. The vast majority of materials degradation problems are, however managed by the former method of coatings and surface modified layers. Most physical phenomena have been applied where possible for the development of coatings and surface modified layers. The power of an explosion has been used to directly clad steel with a corrosion resistant layer of aluminum. Each method of coating or surface modification has its own advantages and disadvantages. For instance, painting may be cheap but will it be effective when the corroding water is substituted by abrasive aqueous slurry. A comprehensive knowledge of the various coating and surface modification techniques is required before an optimum or near-optimum solution to a materials degradation problem can be obtained. A definition of surface engineering is an informed selection of the appropriate coating or surface modification technology and its effective application to prevent or delay one or more forms of materials degradation thereby improving the performance of components and devices.[1]

There are two basic types of surface engineering, providing the substrate with a protective coating and modifying the surface to improve a critical characteristic, e.g. corrosion resistance. Almost every known method of joining two materials together has been considered for adaptation as a method of surface coating. Surface modification is rapidly developing beyond traditional simple processes such as flame hardening to far more advanced solutions to wear, corrosion and fatigue problems.[4]

2.4 TEXTURE

2.4.1 Definition of Texture

Each grain in a polycrystalline aggregate normally has a crystallographic orientation different from that of its neighbors. Considered as a whole, the orientations of all the grains may be randomly distributed in relation to some selected frame of reference, or they may tend to cluster, to a greater or lesser degree, about some particular orientation or orientations. Any aggregate characterized by the latter condition is said to have a preferred orientation, or

texture, which may be defined simply as a condition in which the distribution of crystal orientations is nonrandom. [5]

There are many examples of preferred orientation. The individual crystals in a cold-drawn wire, for instance, are so oriented that the same crystallographic direction [uvw] in most of the grains is parallel or nearly parallel. to the wire axis. In cold-rolled sheet, most of the grains are oriented with a certain plane (hkl) roughly parallel to the sheet surface, and a certain direction [uvw] in that plane roughly parallel to the direction in which the sheet was rolled. These are called deformation textures. Basically, they are due to the tendency, for a grain to rotate during plastic deformation. When a cold-worked metal or alloy, possessed of a deformation texture, is recrystallized by annealing, the new grain structure usually has a preferred orientation too, often different from that of the cold-worked material. This is called an annealing texture or recrystallization texture, and two kinds are usually distinguished, primary and secondary, depending on the recrystallization process involved. Such textures are due to the influence which the texture of the matrix has on the nucleation and/or growth of the new grains in that matrix. The crystallographic texture of the substrate steel is expected to affect the formation and growth behavior of a new phase and during electrodeposition. Preferred orientation can also exist in castings, hot-dipped coatings, evaporated films, electrodeposited layers, etc. [8]

2.4.2 Texture Measurement

Interpretation of textures has to rely on a quantitative description of orientation characteristics. Two types of preferred orientations are distinguished: the lattice preferred orientation (LPO) or ‘texture’ (also ‘preferred crystallographic orientation’) and the shape preferred orientation (or ‘preferred morphological orientation’).

Today diffraction techniques are most widely used to measure crystallographic preferred orientation. X-ray diffraction with a pole-figure goniometer is a routine method. For some applications synchrotron x-rays provide unique opportunities. Neutron diffraction offers some distinct advantages, particularly for large bulk samples. Electron diffraction using the transmission (TEM) or scanning electron microscope (SEM) is gaining interest, because it permits one to correlate microstructures, neighbor relations and texture. [9]

2.4.2.1 X-ray pole-figure goniometer

Preferred orientation is best described by means of a pole figure. This is a stereographic projection which shows the variation in pole density with pole orientation for a selected set of crystal planes. This method of describing textures was first used by the German metallurgist Wever in 1924.

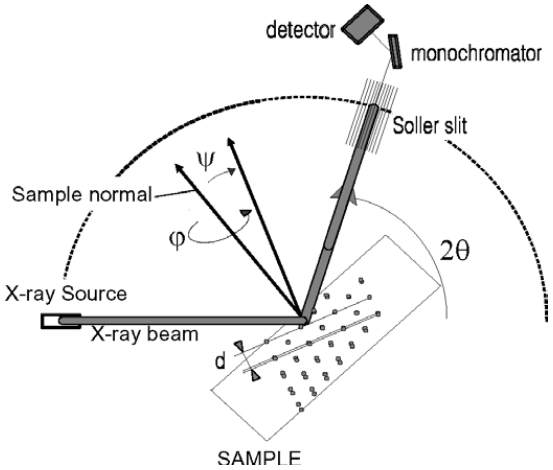

Fig. 2.2 Geometry of a pole-figure goniometer equipped with Soller slits and monochromator[9]

The orientation of any plane in a crystal can be just as well represented by the inclination of the normal to that plane relative to some reference plane as by the inclination of the plane itself. All the planes in a crystal can thus be represented by a set of plane normals radiating from some one point within the crystal. If a reference sphere is now described about this point, the plane normals will intersect the surface of the sphere in a set of points called poles. This procedure is illustrated in Fig.2.3 which is restricted to the {100} planes of a cubic crystal. The pole of a plane represents, by its position on the sphere, the orientation of that plane.

A plane may also be represented by the trace the extended plane makes in the surface of the sphere, as illustrated in Fig. 2.4, where the trace ABCDA represents the plane whose pole is P_1. This trace is a great circle, i.e., a circle of maximum diameter, if the plane passes through the center of the sphere. A plane not passing through the center will intersect the sphere in a small circle.

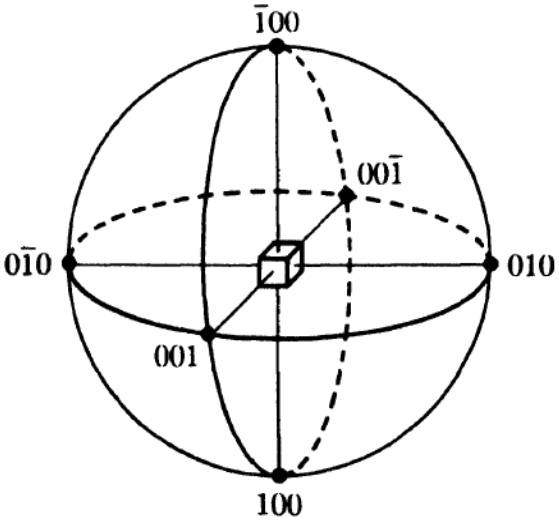

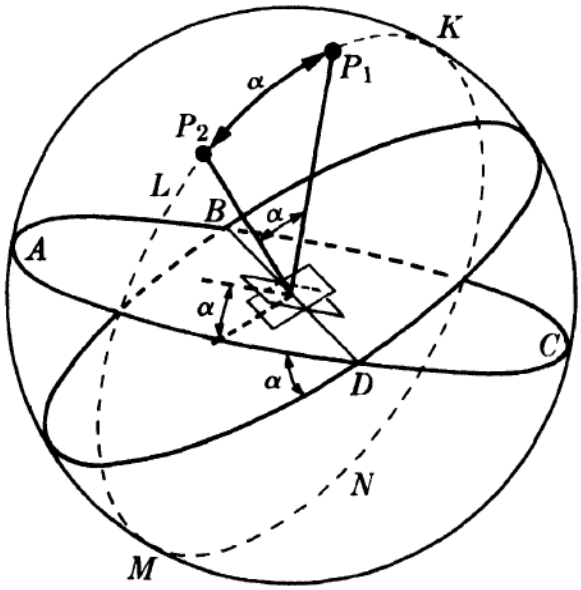

Fig. 2.3 {100} poles of a cubic Fig. 2.4 Angle between two planes

In crystallography, however, we prefer the equiangular stereographic projection since it preserves angular relationships faithfully although distorting areas. It is made by placing a plane of projection normal to the end of any chosen diameter of the sphere and using the other end of that diameter as the point of projection.

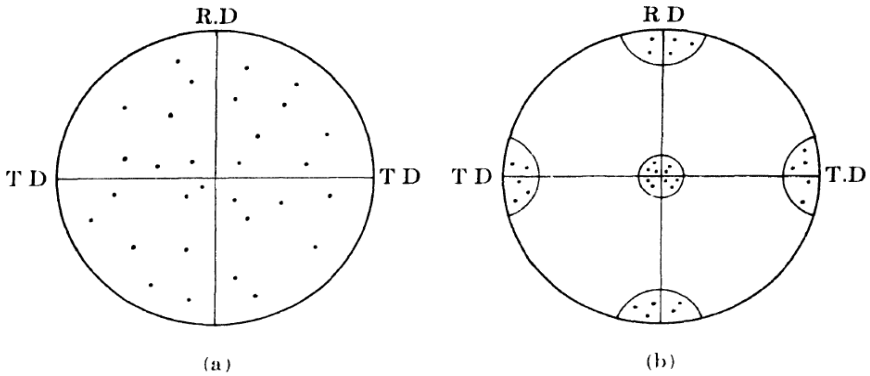

Fig. 2.5 (100) pole figures for sheet material, illustrating (a) random orientation and (b) preferred orientation. R.D. (rolling direction) and T.D. (transverse direction) are reference directions in the plane of the sheet.

The meaning of Pole Figure can best be illustrated by the following simple example. Suppose we have a very coarse-grained sheet of a cubic metal containing only 10 grains, and that we

determine the orientation of each of these 10 grains by one of the Laue methods. We decide to represent the orientations of all of these grains together by plotting the positions of their {100J poles on a single stereographic projection, with the projection plane parallel to the sheet surface. Since each grain has three {100} poles, there will be a total of 3 X 10 = 30 poles plotted on the projection. If the grains have a completely random orientation, these poles will be distributed uniformly over the projection, as indicated in Fig. 2.5 (a). But if preferred orientation is present, the poles will tend to cluster together into certain areas of the projection, leaving other areas virtually unoccupied. For example, this clustering might take the particular form shown in Fig. 2.5(b). This is called the "cube texture" because each grain is oriented with its (100) planes nearly parallel to the sheet surface and the [001] direction in these planes nearly parallel to the rolling direction. [5]

2.4.2.2 Synchrotron x-rays

A synchrotron enables production of fine-focused high-intensity beam of x-rays with monochromatic or continuous wavelengths. However conventional X-rays produce a broad beam of relatively lower intensity (~1mm). The unique advantages of high intensity, small beam size (<5 μm) and free choice of wavelength open a wide range of new possibilities. Synchrotron diffraction images recorded by CCD detectors almost instantaneously display the presence of texture expressed in systematic intensity variations along Debye rings. The presence of texture is immediately obvious, while elaborate data processing is necessary to determine texture patterns quantitatively and interpret data in a satisfactory way.

2.4.2.3 Neutron diffraction

Neutron diffraction texture analysis is almost as old as the pole-figure goniometer. It was first applied by Brockhouse (1953) in an attempt to determine magnetic structure in steel. Neutron diffraction texture studies are done either at reactors with a constant flux of thermal neutrons, or with pulsed neutrons at spallation sources. The wavelength distribution of thermal neutrons is a broad spectrum with a peak at 1–2 A, similar to x-rays. A disadvantage of neutrons is that the interaction of neutrons with matter is low, and long counting times are required. Weak interaction is also a great advantage because it provides high penetration and low absorption, making neutrons suitable for bulk texture investigations of large sample volumes. Because of the low absorption, environmental stages (heating, cooling, straining) can be used for *in situ* observation of texture changes, e.g. during phase transformations.

Neutrons are also sensitive to measuring the orientation of magnetic dipoles, but though this was the original incentive for Brockhouse, to this day no satisfactory magnetic pole figures have been measured.

2.4.2.4 Transmission electron microscope (TEM)

The TEM offers excellent opportunities to study textural details in fine-grained aggregates. Like light microscopy, the TEM not only provides information about orientation but also about grain shape and, more importantly, about dislocation microstructures indicative of active deformation mechanisms.

2.4.2.5 Scanning electron microscope (SEM)

Local orientations can also be measured with the SEM and this technique is becoming very popular because it does not require much background in texture theory from the user. Local orientations can also be measured with the SEM and this technique is becoming very popular because it does not require much background in texture theory from the user (e.g. Randle and Engler (2000)). Unlike the TEM, the SEM is not restricted to thin areas located along the edge of a hole in a small specimen (<2 mm), but enables crystal orientations to be determined on surfaces of considerable extent. Interaction of the electron beam with the uppermost surface layer of the sample produces electron back-scatter diffraction patterns (EBSPs or EBSD) that are analogous to Kikuchi patterns in the TEM. **[9]**

2.5 Surface Coating of Metals

We can protect a surface from environmental attack, by application of an organic, inorganic or metallic coating, so extending the life of not just the surface, but the entire component or equipment. The coating processes shown in Fig. 2.6 serve to illustrate the diversity of available and economically important processes which are commercially available and can be used to protect surface functionality and so extend the life of the component or equipment in question.

Whatever coating technique is used, it is almost invariably necessary to use the appropriate pretreatment and cleaning of the surface to maximise the performance of the coating.[2]

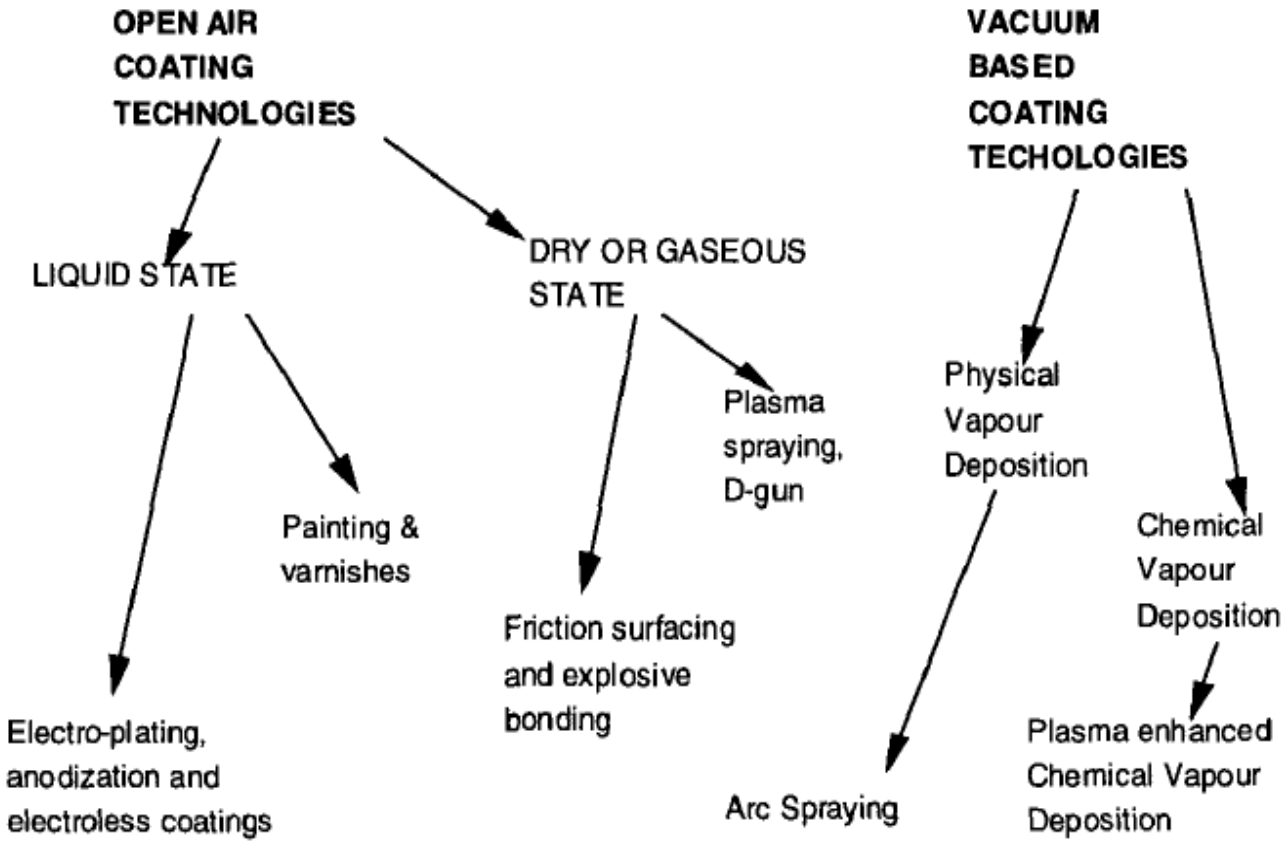

Fig. 2.6 Classification of the different types of discrete coating technologies [1]

2.5.1 Electroplating

If a metal object is placed in an aqueous solution of a salt of the same metal or a different metal and supplied with a strong cathodic electric potential, electroplating of the metal object may occur. Electroplating is caused by cathodic reactions leading to the reduction of metal from solution and evolution of hydrogen or oxygen. Typical examples of electroplating mostly involve iron or steel as the substrate and metals such as nickel, chromium and cadmium as the plating metal. Electroplating is performed in large tanks of metal salt solution with an attached power supply and immersed lead sheet that functions as the anode. The range of metals that can be electroplated is limited and electroplating of metal alloys presents considerable difficulty. The formation of a metal film on a substrate from metal ions in aqueous solution is a complex process that is still not fully understood. In most instances, this film formation process functions well without external intervention and is therefore usually overlooked. It is generally believed that electroplated coatings begin as small nodules of deposited metal, which then grow laterally to form a coating. The coating contains flaws at

the boundary where the growth of one nodule joins the growth of another nodule. The principle of electroplating and structure of electroplated coatings are illustrated schematically in figure.

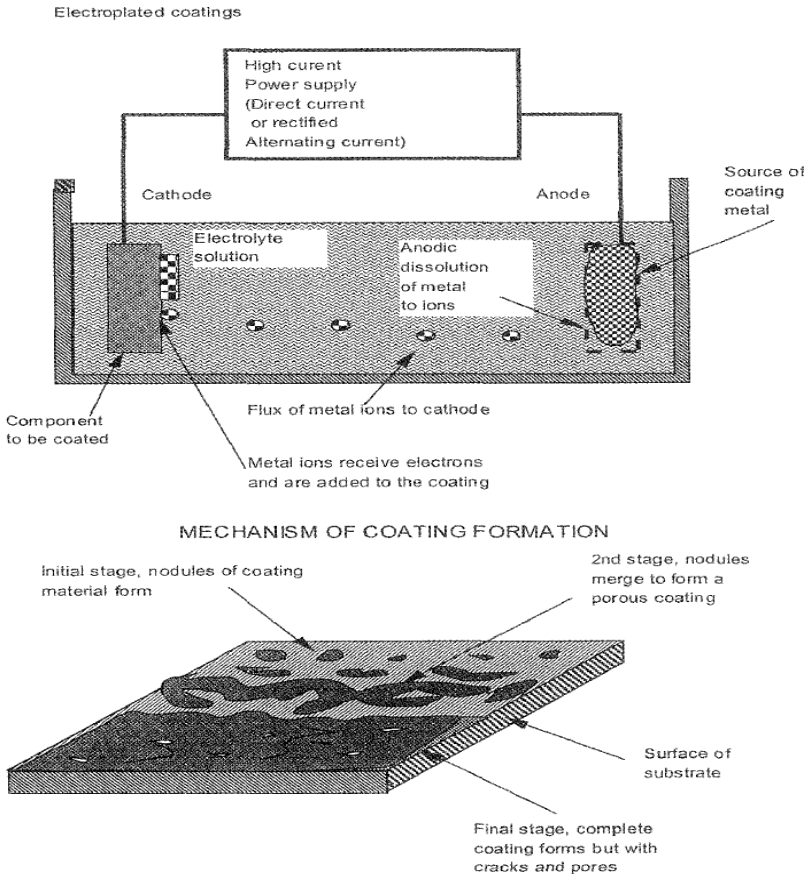

Fig. 2.7 Mechanism of electroplating and structure of electroplated coatings

In electrowinning, a current is passed from an inert anode through a liquid *leach* solution containing the metal so that the metal is extracted as it is deposited in an electroplating process onto the cathode. In electrorefining , the anodes consist of unrefined impure metal, and as the current passes through the electrolyte the anodes are corroded into the solution so that the electroplating process deposits refined pure metal onto the cathodes.

Electroplated coatings tend to be rich in hydrogen from the cathodic reactions and the hydrogen can often cause microstructure problems in the electroplated coating such as brittleness. Another problem of electroplated coatings is non-uniformity of coatings. Electroplating is dependent on the local strength of electric field between anode and cathode and varies with location in an electroplating cell. Corners, edges and projections generate the most intense electric field and so are coated more rapidly than plane surfaces. Practical

considerations dictate a uniform coating time for all parts of an electroplated substrate with the result that thick coatings are formed at edges, corners and projecting parts of the component. A recent development in electroplating tries to combine the advantages of oldest method of electroplating and the conventional method described above. The older method uses spontaneous redox reactions to deposit a film on both insulating surfaces and metallic surfaces and the control of deposition conditions are difficult. The recently developed electroplating technique permits coating of insulating substrates with metals having controlled grain size, thickness and growth speed. The method uses progressive outward growth of the metal from an electrode in contact with the substrate, with the cell geometry chosen so that the electron current providing the reduction passes through the growing deposit. [1]

2.5.1.1 Nickel Plating

Nickel coatings are most widely used for their high corrosion resistance, coupled with an attractive visual appearance. Thus, taps and sanitaryware, automotive components and light fittings are but a few examples of this widely used coating. The metallising of plastics using nickel, gives such components a metallic appearance, a higher reflectivity and low weight- a valuable combination of properties. In electroforming too, nickel coatings are widely used for their higher hardness, wear- and corrosion-resistance.[2]

Nickel plating is similar to other electroplating processes that employ soluble metal anodes. It requires the passage of direct current between two electrodes that are immersed in a conductive, aqueous solution of nickel salts. The flow of direct current causes one of the electrodes (the anode) to dissolve and the other electrode (the cathode) to become covered with nickel. The nickel in solution is present in the form of divalent positively charged ions (Ni+). When current flows, the positive ions react with two electrons (2e-) and are converted to metallic nickel (Ni0) at the cathode surface. The reverse occurs at the anode where metallic nickel is dissolved to form divalent positively charged ions which enter the solution. The nickel ions discharged at the cathode are replenished by those formed at the anode.[7]

Electroplating is the most widely used method of nickel plating. The following solutions are used for nickel electroplating:

- Watts nickel plating solutions

- Nickel sulfamate solutions
- All-Chloride solutions
- Sulfate-Chloride solutions
- All-Sulfate solutions
- Hard nickel solutions

Nickel electroplating is a process of nickel deposition on a part, immersed into an electrolyte solution and used as a cathode, when the nickel anode is being dissolved into the electrolyte in form of the nickel ions, traveling through the solution and depositing on the cathode surface. [6]

The following Table 2.1 shows the various Electroplating Solutions: [7]

Table 2.1

	Electrolyte Composition[1], g/L		
	Watts Nickel	Nickel Sulfamate	Typical Semi-Bright Bath[2]
Nickel Sulfate, $NiSO_4 6H_2O$	225 to 400		300
Nickel Sulfamate, $Ni(SO_3NH_2)_2$		300 to 450	
Nickel Chloride, $NiCl_2 6H_2O$	30 to 60	0 to 30	35
Boric Acid, H_3BO_3	30 to 45	30 to 45	45
	Operating Conditions		
Temperature, ^0C	44 to 66	32 to 60	54
Agitation	Air or mechanical	Air of mechanical	Air or mechanical
Cathode Current Density, A/dm^2	3 to 11	0.5 to 30	3 to 10
Anodes	Nickel	Nickel	nickel
PH	2 to 4.5	3.5 to 5.0	3.5 to 4.5
	Mechanical Properties		
Tensile Strength, Mpa	345 to 485	415 to 610	-
Elongation, %	10 to 30	5 to 30	8 to 20
Vickers Hardness, 100 gram load	130 to 200	170 to 230	300 to 400
Internal Stress, Mpa	125 to 185 (tensile)	0 to 55 (tensile)	35 to 150 (tensile)

NOTE 1 Anti-pitting agents formulated for nickel plating are added to control pitting.
NOTE 2 Organic additives available from plating supply houses are required for semibright nickel plating.
NOTE 3 Typical properties of *bright* nickel deposits are as follows: Elongation, % - 2 to 5 Vickers Hardness,100 gram load - 600 to 800; Internal Stress, MPa - 12 to 25 compressive.

2.5.1.2 Chromium Plating

Electroplated chromium coatings are notable for their high resistance to tarnish, their high hardness and wear resistance as well as their low coefficient of friction resistance to cold welding. With a thickness of 0.2-0.6 µm and bright silver to matt appearance, they are widely used as decorative finishes. Thus, special design effects can be achieved. [2] Chromium plating is performed with a chromium salt solution and a passive anode made of lead. Trivalent chromium solutions are limited to low deposition rates and are mainly used for the

deposition of thin decorative coatings. Hexavalent chromium solutions provide higher deposition rates than trivalent chromium solutions and are used for the production of thick wear-resistant hard chromium coatings. Chromium solutions are used in high concentrations and at an elevated temperature of 50 to 80 °C in order to achieve rapid coating concentrations, e.g. 250 g of chromium oxide per liter of sulfuric acid solution. Current densities are of the order of 100 Amperes per square meter for fast plating of chromium. [1]

Hexavalent chromium (Cr^{6+}) baths are used for hard chromium deposition. The main component of all hard chromium plating solutions is chromium trioxide (CrO_3) referred also as chromic acid. The second component is a catalyst, which is either sulfate (SO_4^{2-}) or fluoride.

By-product of the electroplating process in hexavalent chromium solutions is trivalent chromium (Cr^{3+}). Ions of trivalent chromium continuously reoxidize to the hexavalent state at the anode. Normal level of the trivalent chromium is about 1-2% of the chromic acid concentration. Higher contents of trivalent chromium may cause reduction of throwing power and plating rate, pitting and treeing of the deposit. If the trivalent chromium is too high (more than 2%) reoxidation operation should be carried out at high anode area/cathode area ratio (30) at cathode current density 20 A/ft² (2A/dm²).

Cathode current efficiency of hard chromium electroplating is low: about 10-20%. 80-90% of the electric current passing between the anode and the cathode is used for gaseous Hydrogen formation.

Conventional hard chromium plating process

In this process chromic acid is catalyzed by sulfate ions (SO_4^{2-}). Chromic acid/sulfate ratio is one of the most important process parameters. It varies within the range 125 - 200. Low ratio solutions are characterized by high plating rate but low throwing power. High chromic acid/sulfate ratio may cause gray or even “burnt” deposition on high current density areas. Normally plating solutions with chromic acid/sulfate ratio 155 are used.

*Bath formulation:*Chromic acid (CrO_3): 20-35 oz/gal (150-263 g/l); Sulfate (SO_4^{2-}): 0.13-0.23 oz/gal (1-1.73 g/l). Source of sulfate ions is sulfuric acid.

Hard chromium plating in fluoride bath:

In this process chromic acid is catalyzed by a mixture of sulfate and fluoride ions. Fluoride bath have higher than sulfate baths current efficiency. Additionally fluoride baths may operate at higher current density not causing burning and treeing. As a result plating rate in fluoride baths may be 50% higher than in conventional sulfate catalyzed baths. Fluoride ions are chemically active and may attack the unplated surfaces. In order to prevent etching of the areas, which are not to be plated, they should be masked.[7]

While chromium deposits from hexavalent electrolytes are silver with a blueish tinge, those formed from trivalent chromium baths can have an attractive smoky appearance. Black chromium deposits can also be formed, and a thickness from 0.5 to 2.0 ~m is often used for optical equipment and cameras. In contrast to decorative chromium, hard chromium deposits are usually much thicker, from 10 to 500 µm. They are typically applied to cylinder bores, valves and piston rods of diesel locomotive engines. [2]

Chromium plating is prone to cracking where the plating thickness is greater than 0.5 nm and it is believed that cracking is caused by the formation of chromium hydride, which later decomposes to pure chromium. The density of pure chromium is higher than chromium hydride so that shrinkage cracks result. The physical structure of chromium plating consists of metal grains separated by small pores and fissures. This structure results from the mechanism of formation of chromium plating where granules of chromium independently grow to cover the substrate. The hardness of chromium plating can reach 1000 Hv hence its used as a wear resistant coating. A major problem with chromium electroplating which is predicted to severely restrict its future usage is toxicity. Inorganic compounds of either trivalent chromium or hexavalent chromium are used as the source of chromium. Trivalent and hexavalent chromium ions are toxic and hexavalent chromium is carcinogenic while the lead anode is also toxic. There are health risks to electroplating personnel and problems with disposal of liquid and solid waste from electroplating. Hard chromium coatings are effective as antiwear coatings but no more so than the more recently developed coatings produced by vacuum and plasma technology. [1]

2.6 Steels

Thousands of different steel compositions are available in the market and there are numerous ways one may classify steels. Generally, the carbon and low-alloy steels come under a classification system based on composition. The higher-alloy steels (the stainless, heat-resistant, wear-resistant steels, etc.) can be classified according to many different systems, including composition, microstructure, application, or specification. The easiest way to classify steels is by their chemical composition.

Various alloying elements are added to iron for the purpose of attaining certain specific properties and characteristics. These elements include, but are not limited to, carbon, manganese, silicon, nickel, chromium, molybdenum, vanadium, columbium (niobium), copper, aluminum, titanium, tungsten, and cobalt. The steels used in our experiment are mentioned below. These steels are highly formable and easily develop texture. They find wide application especially in automobile industry.

2.6.1 Interstitial Free Steel (IF)

This steel consists of strong carbide forming elements such as Titanium and Niobium so that very little carbon is left in solid solution. They have ultra low carbon content, well below 0.005%.The IF steels find application in automobile industry.[13] The steel is virtually cementite-free and the microstructure is almost 100% ferritic. These steels display good deep drawing behavior and are best suited for continuous annealing and hot-dip galvanizing processes.[10]

2.6.2 High Strength Interstitial Free Steels (HIF)

HIF steel is the high strength version of interstitial free steels obtained through additions of manganese and phosphorous. These produce solid solution strengthening without any loss of formability. HIF steels too find application in automobile industry as automotive body panels where strength is a major issue. However as per the recent report, deterioration in formability has been noticed in these steels.

2.6.3 Bake Hardening Steels (BH)

BH steel is also of high importance to the automobile industry. The dent resistance of the steel is appropriately increased after baking. During Baking, the interstitial C, N atoms diffuse rather quickly into free dislocations and fix them, thereby raising the yield strength of steel and obtaining baking hardening.[14]

2.6.4 Extra Deep Drawing Steels (EDD)

The exterior components such as petrol tanks, starter end covers, etc. are made of these types of steels.EDD steels are used in applications involving simple to complex stampings which require very high formability, mainly stretchability and drawability. They exhibit high resistance to thinning during drawing. [11]

3. Experimental

3.1 Coating of Steel Samples

3.1.1 Sample Details

The four different steel samples used in our experiment were provided by Tata Steel, Jamshedpur. The samples were rolled (textured) and their rolling direction was mentioned. The details of the samples are:

- **Bake Hardening Steel:**
  Composition - % C: 0.002; % Si: 0.015; % Mn: 0.40; % Al: 0.05 (max); %S: 0.01(max); % P: 0.04; and balance Fe (in wt.%).
  Finish Roll temperature: 900^{o}C
  Coiling temperature: 570^{o}C
  Annealing temperature: 710^{o}C

- **Extra Deep Drawing Steel:**
  Composition - % C: 0.05; % Si: 0.015; % Mn: 0.20; % Al: 0.06 (max); %S: 0.01(max); % P: 0.015; and balance Fe (in wt.%).
  Finish Roll temperature: 900^{o}C
  Coiling temperature: 550^{o}C
  Annealing temperature: 685^{o}C

- **High Strength Interstitial Free Steel:**
  Composition - % C: 0.0035; % Si: 0.015; % Mn: 0.65; % Al: 0.02 (min); % Ti: 0.07; % Nb: 0.02; %S: 0.01(max); % P: 0.04; and balance Fe (in wt.%).
  Finish Roll temperature: 910^{o}C
  Coiling temperature: 720^{o}C
  Annealing temperature: 680^{o}C

- **Interstitial Free Steel:**
  Composition - % C: 0.0035; % Si: 0.015; % Mn: 0.15; % Al: 0.06 (max); % Ti: 0.04; % Nb: 0.02; %S: 0.01(max); % P: 0.018; and balance Fe (in wt.%).
  Finish Roll temperature: 900^{o}C

Coiling temperature: 700^{o}C

Annealing temperature: 700^{o}C

3.1.2 Sample Preparation

- Five rectangular pieces of each of the above mentioned rolled steels were cut out from the sheets using hack saw.

- The dimension of the rectangular pieces was approximately 2 cm × 1.5 cm. Care was taken to avoid any significant texture changes in the steel samples while cutting.

- The rolling direction of each of the rectangular pieces was noted down carefully. These steel pieces were then polished to remove rust, dirt on the surface.

3.1.3 Electroplating Solution Preparation

- As mentioned earlier in the Literature Review part (2.5.1.1), electroplating solution for deposition of Nickel and Chromium coating on the rectangular pieces cut earlier was prepared. Magnetic stirrer was used to obtain a uniform solution for electroplating of both Ni and Cr.

- Watts bath is used for deposition of Nickel. A solution consisting Nickel Sulphate (350 g/l), Nickel Chloride (45 g/l), Boric Acid (37 g/l) was used.

- For Chromium plating, Chromic Acid solution (CrO_3) with addition of H_2SO_4 was used

Table 3.1

	Nickel Electroplating	Chromium Electroplating
Solution	Watts Bath	Chromic Acid Bath
Current	0.29 A (5 A/dm^2)	3.36 A (20-70 A/dm^2)
Voltage	~ 1.9 V	~ 5 V
Temperature	~ 54 º C	57 º C
Time (minutes)	20	40
Mode	Constant Current Mode	

3.2 Characterisation

3.2.1 X-Ray Diffraction (XRD)

- The surface microstructure were analyzed by Bragg-Brentano (theta-2theta) x-ray diffraction (XRD) using Cu K_α (α = 0.15406 nm) radiation for both the coated and uncoated samples.
- Texture analysis of the surfaces was carried out in a fully automatic x-ray texture goniometer using Scultz reflection method [5] in the range α = 20-100^o. From the accumulated data (110) pole figures for uncoated steel (BCC α-Fe) as well as for Cr coated steel (BCC Cr) were drawn using Philips X'pert software. For Ni coated steel samples (200) pole figures were obtained (FCC Ni) using the same software. Details discussion about pole figure is already covered in literature review [2.4.2.1].

X-ray diffraction is a tool for the investigation of the fine structure of matter. [5] At first, x-ray diffraction was used only for the determination of crystal structure. Later on, however, other uses were developed, and today the method is applied, not only to structure determination, but to such diverse problems as chemical analysis and stress measurement, to the study of phase equilibria and the measurement of particle size, to the determination of the orientation of one crystal or the ensemble of orientations in a polycrystalline aggregate. It discloses the various compounds and phases present in the sample. [12]

3.2.2 Scanning Electron microscope (SEM)

- Microstructures of uncoated and coated steel surface were examined using optical as well as scanning electron microscope (SEM). For proper observation under microscope, uncoated samples were etached with 2% natal.

The scanning electron microscope (SEM) uses a focused beam of high-energy electrons to generate a variety of signals at the surface of solid specimens. The signals obtained from electron-sample interactions reveal information about the sample including external morphology (texture), chemical composition, and crystalline structure and orientation of materials making up the sample.

3.2.3 Microhardness Measurement

Microhardness measurements were carried out on the surface of the coated and uncoated samples using a Vickers hardness indenter with 50 g load.

3.3 Overview of Experimental Procedure

Small rectangular pieces of 2cm × 1.5cm were cut out from the rolled IF and EDD Steel samples. Care was taken to avoid any significant texture changes while cutting.

↓

Two samples of each type of steel were plated with Nickel. The Solution used was Nickel Watts bath consisting of Nickel Sulfate, Nickel Chloride, Boric Acid. Current Density was 5 A/dm^2

↓

Two samples of each type of steel were plated Chromium. The electroplating solution consisted of Chromic Acid and Sulfate ions. Current Density was 20-70 A/ dm^2

↓

These electroplated samples would be subjected to texture measurement, XRD, SEM analysis and hardness measurement.

4. Result and Discussion

4.1 X-ray Diffraction

4.1.1 Phase Analysis

Figure 4.1 shows XRD profile of four different uncoated steel samples. All the profiles exhibit only α–Fe peaks as these steels contain almost entirely ferrite phase.

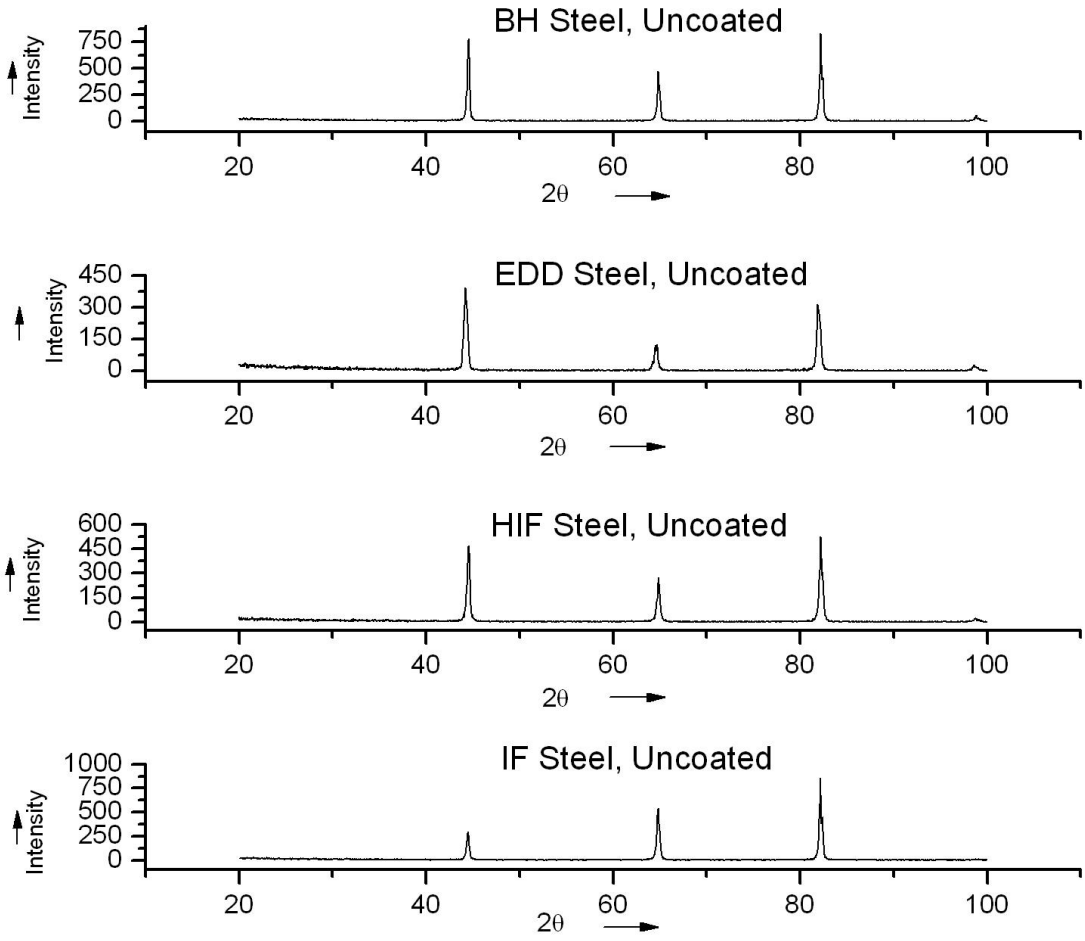

Figure 4.1: XRD profiles of uncoated steels

In figure 4.1 it can be observed that different peaks corresponding to different planes are changing relatively from steel to steel. This can be due to presence of preferred orientation.

To analyze this, relative intensity of first two planes i.e. (110) and (200) are being analyzed and their normalized intensities are shown in Table 4.1 given below. To get a graphical idea the change of relative intensity of (200) plane of different steels are shown in the bar chart

(Fig. 4.2). In Fig 4.2, it can be observed that the relative intensity is changing and deviating from the theoretical value obtained from JCPDS data. The Fig. also shows that IF steel's (200) intensity is maximum and EDD steel is minimum.

Table 4.1: Intensity variation of different planes of uncoated steels

Uncoated Steel Samples				
	Measured (cts)		Normalized (%)	
	(110)	(200)	(110)	(200)
Theoretical Value	--	--	100	20
BH Steel	762.34	424.62	100	55.70
EDD Steel	386.61	102.94	100	26.63
HIF Steel	468.83	244.08	100	52.06
IF Steel	285.35	525.23	100	184.06

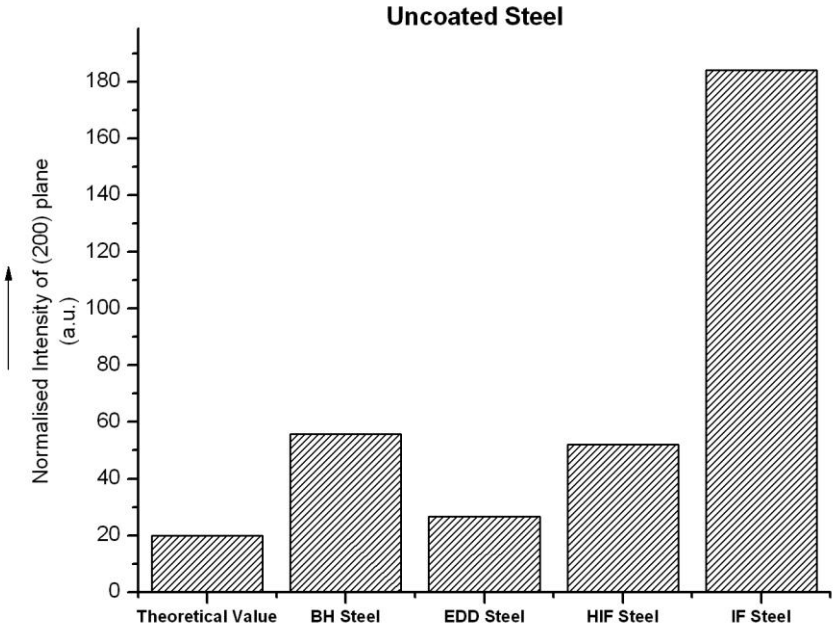

Figure 4.2: (200) plane intensity variation of uncoated steels

The Fig. 4.3 given below shows the XRD profile of 4 different Chromium coated steel samples. Chromium peaks can be seen in all the profiles as all the steels are coated with chromium.

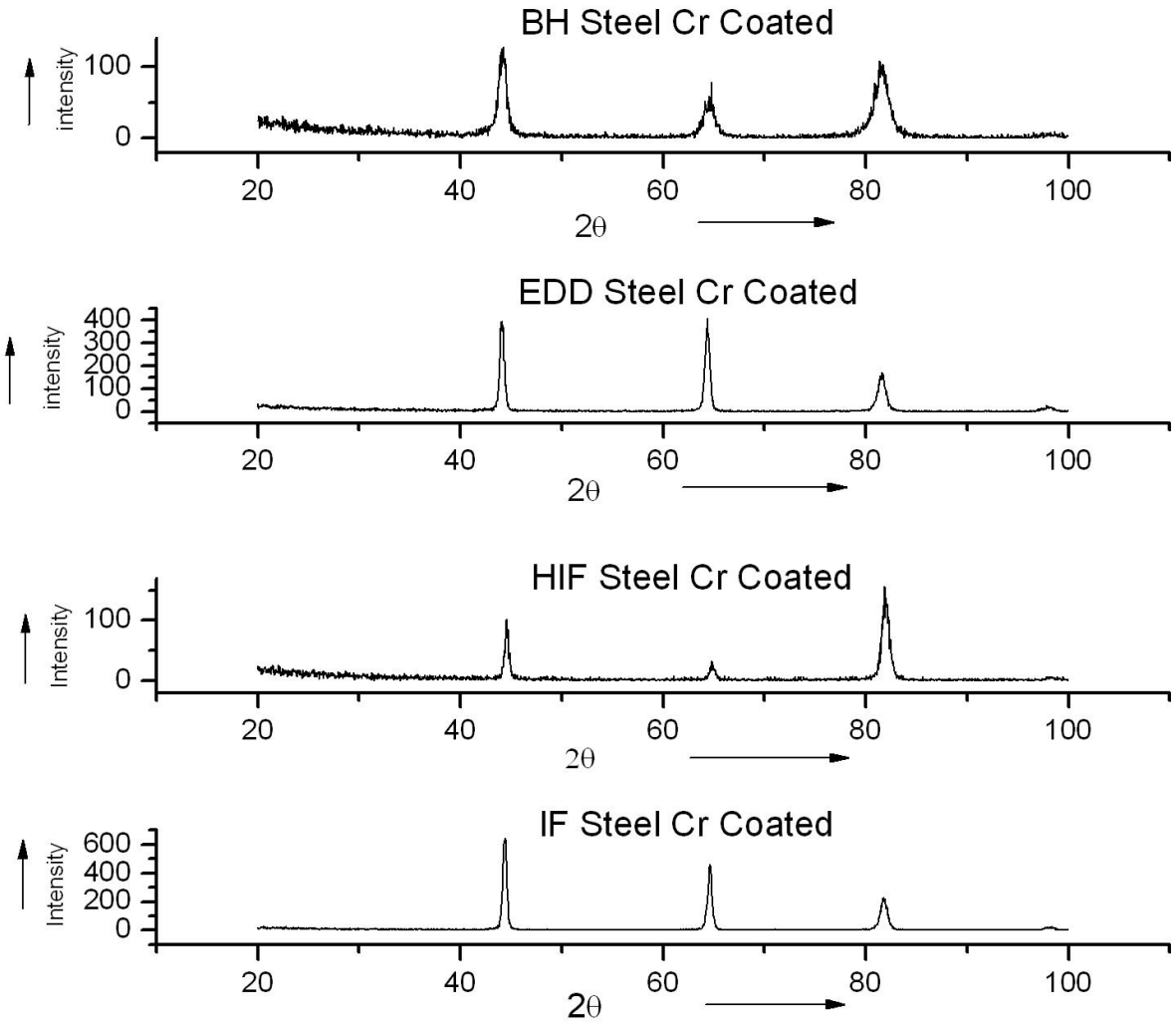

Figure 4.3: XRD profiles of Cr-coated steels

It can be seen from the Fig. 4.3, the peaks of a particular plane obtained are of different intensity for different steel samples. This may be a result of presence of preferred orientation in the sample.

The relative intensity of (110) and (200) planes i.e. the first two planes are being analysed to determine this change. The normalized intensity of these planes with their relative intensity is shown in Table 4.2. To get a graphical idea the change of relative intensity of (200) plane of different Chromium coated steels are shown in bar chart (Fig 4.4). In Fig. 4.4 it can be observed that normalized intensity is changing and deviating from the theoretical value obtained from JCPDS data. The Fig. also shows that EDD steel's (200) intensity is maximum and HIF steel is minimum.

Table 4.2: Intensity variation of different planes of Cr-coated steels

Cr coated Steel Samples				
	Measured (cts)		Normalized (%)	
	(110)	(200)	(110)	(200)
Theoretical Value	--	--	100	16
BH Steel	102.10	46.69	100	45.73
EDD Steel	344.57	374.65	100	108.73
HIF Steel	89.03	23.35	100	26.23
IF Steel	638.37	456.67	100	71.54

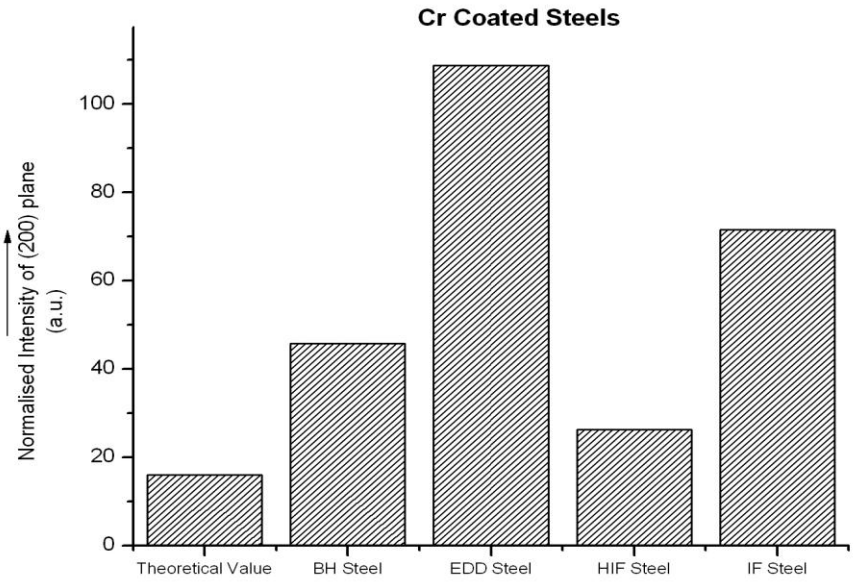

Fig. 4.4: (200) plane intensity variation of Cr-coated steels

Fig. 4.5 shows XRD profile of Nickel coated samples of BH Steel, EDD Steel, HIF Steel and IF Steel. All the profiles exhibit only Ni peaks as these steels are coated with Nickel.

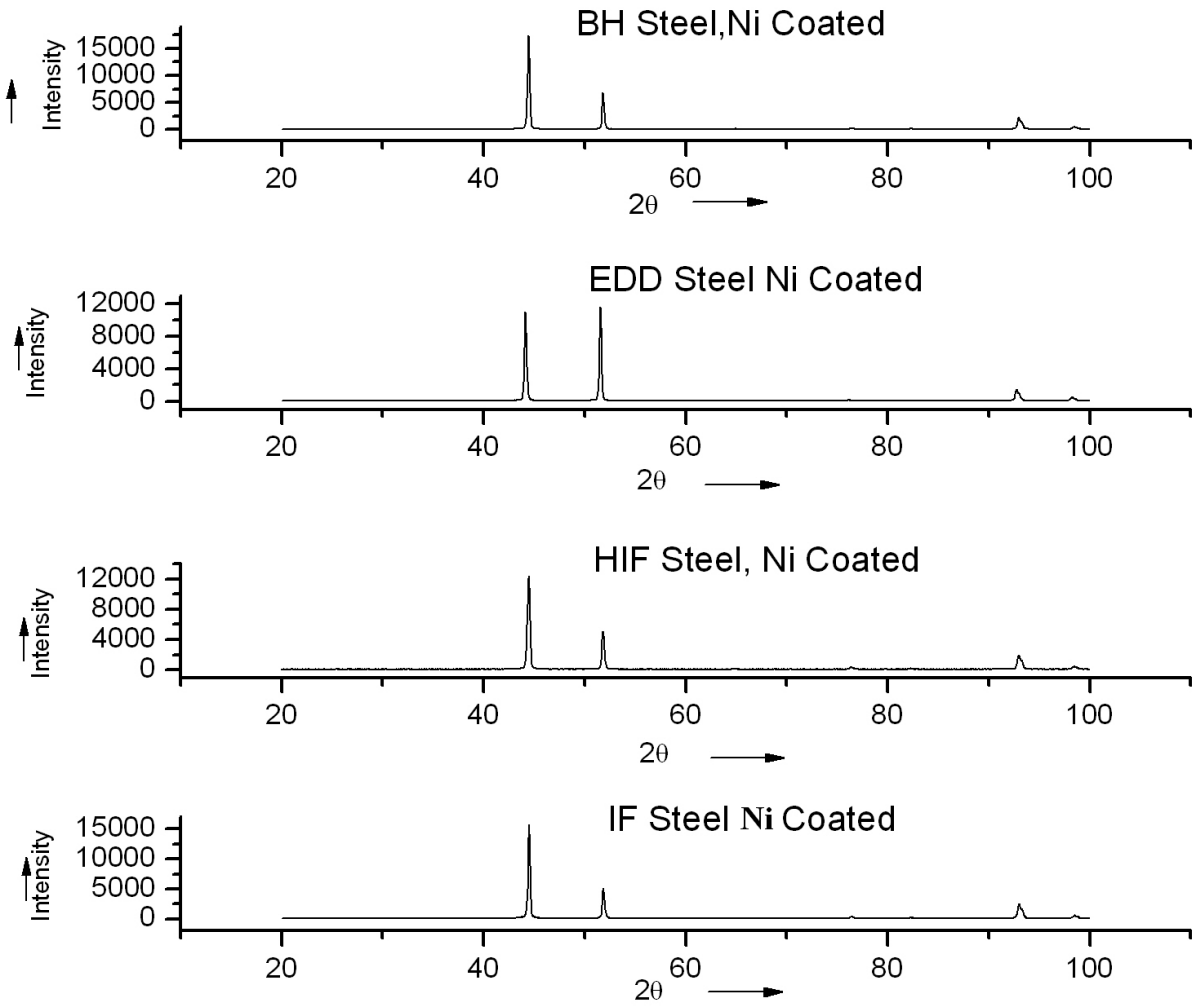

Fig. 4.5: XRD profiles of Ni-coated steels

In Fig. 4.5, it can be observed that different peaks corresponding to different planes are changing relatively from steel to steel. This may be a result of preferred orientation introduced in the sample by mechanical working.

This is analyzed by measuring the relative intensity of first two planes i.e. (111) and (200).The normalized intensities are shown in Table 4.3 given below. To get a graphical idea the change of relative intensity of (200) plane of different Nickel coated steels are shown in the bar chart (Fig. 4.6). In Fig 4.6, it can be observed that the relative intensity is changing

and deviating from the theoretical value obtained from JCPDS data. The Fig. also shows that EDD steel's (200) intensity is maximum and IF steel is minimum.

Table 4.3: Intensity variation of different planes of Ni-coated steels

Ni coated Steel Samples				
	Measured (cts)		Normalized (%)	
	(111)	(200)	(111)	(200)
Theoretical Value	--	--	100	42
BH Steel	17317.39	6749.94	100	38.98
EDD Steel	10991.08	11356.74	100	103.32
HIF Steel	12166.26	5010.38	100	41.18
IF Steel	15514.89	4951.96	100	31.92

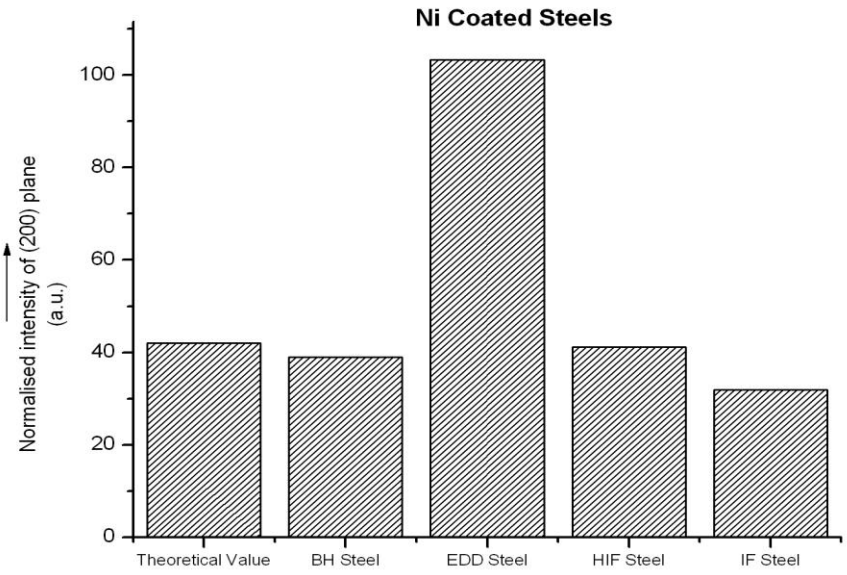

Fig. 4.6: (200) plane intensity variation of Ni-coated steels

In general it was observed that coated EDD steel (both Ni and Cr) shows maximum (200) intensity whereas uncoated IF steel shows maximum (200) intensity among uncoated samples. To analyze the detailed texturing effect pole figure measurement was carried out.

4.1.2 Pole Figure

In the earlier section some rough idea about the texturing of the present specimen was obtained. To further analyze it, Pole figure were measured for all the samples (coated and uncoated) on particular plane of importance.

Fig. 4.7 shows (110) pole figure of uncoated and Chromium coated steels. For uncoated steels, (110) plane corresponds to α-Fe plane, whereas, for Chromium coated steel it is on (110) plane of coated Chromium (both are Body Centered Cubic).

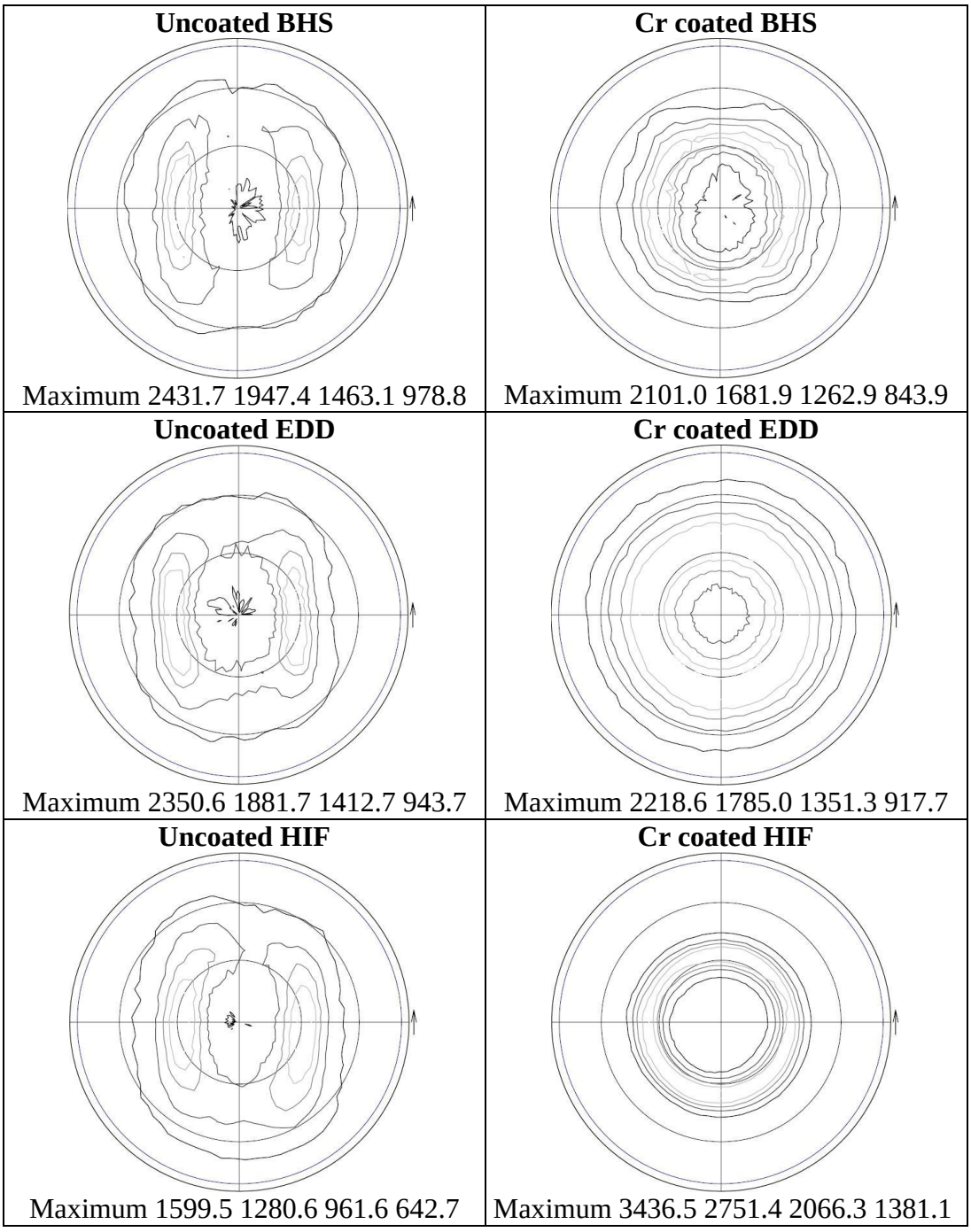

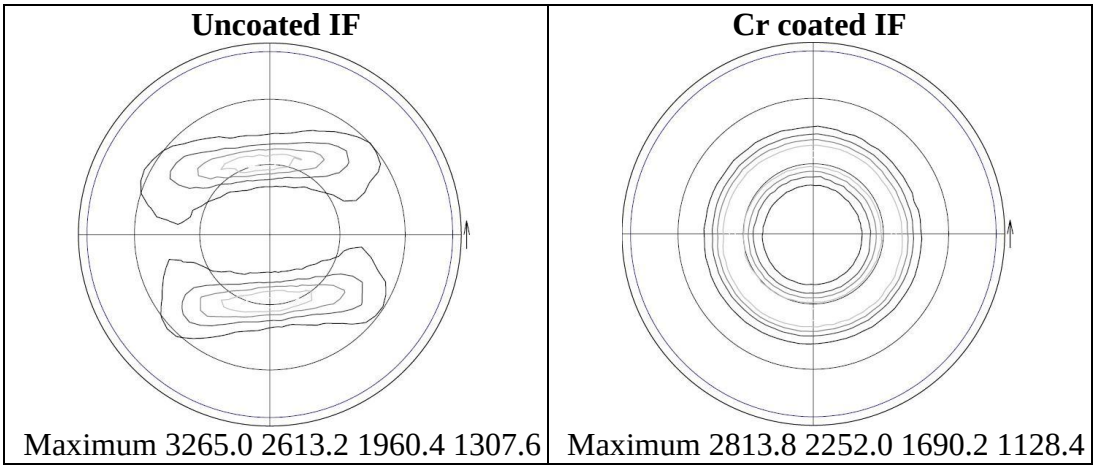

Fig 4.7: (110) pole figure of uncoated steel and Cr coated samples

Figure 4.7 shows that uncoated steel have weak texture and except IF steel, other have similar one. After chromium coating, as per the (110) oile figure the texture is further weaker. All the four steels after Chromium coating show same type of pole figure even for IF steel.

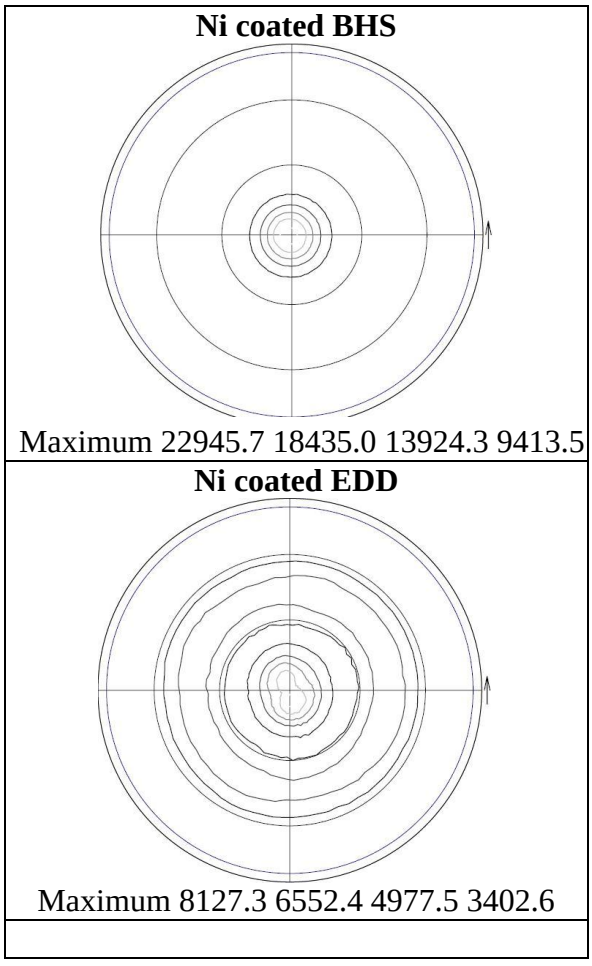

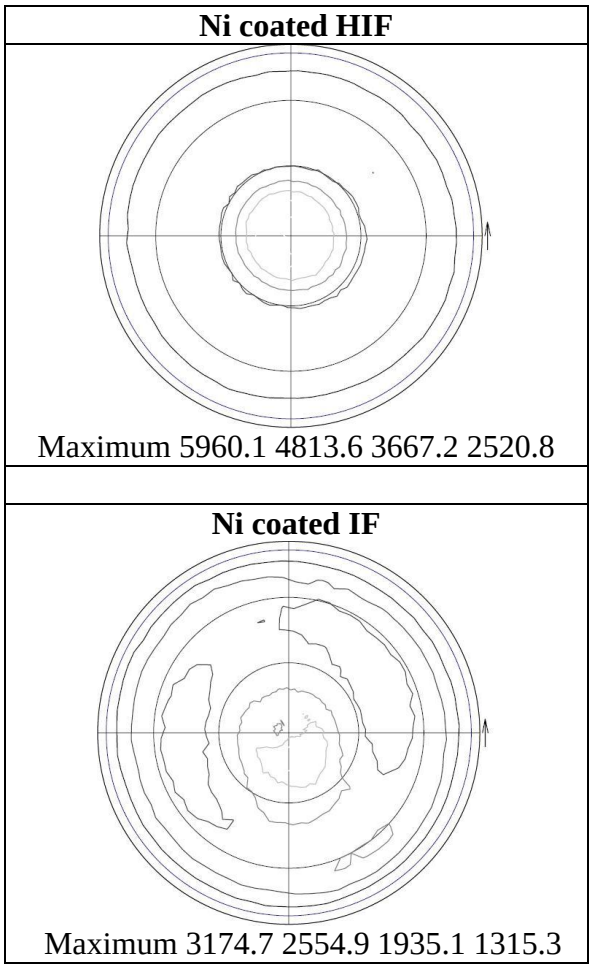

Fig 4.8: (200) pole figure of Ni coated samples

Fig. 4.8 shows (200) pole figure of Ni coated steels measured on (200) plane of Nickel (Face centered cubic). In this figure, except IF steel, others show almost no texturing. Ni coated IF steel shows weak texture only. Different trend in Ni coated IF Steel may be due to different substrate texture of the IF steel as shown earlier in Fig. 4.7.

In the case of Nickel coating, only for IF steel, some effect of substrate texture can be observed but not for Chromium coated samples. So, it can be concluded that in the present study, the effect of substrate texture is almost negligible on coating. This may be due to the thickness of Chromium and Nickel coating. From the coating time, it can be estimated that the thickness was 10 to 15 micron which can eliminate substrate texture effect on the coating surface outer layer.

4.2 Microstructure Analysis

Fig. 4.9-4.12 show SEM photograph of four different uncoated steels. All the microstructures show mainly ferrite grains. In some samples grain boundary was clearly visible.

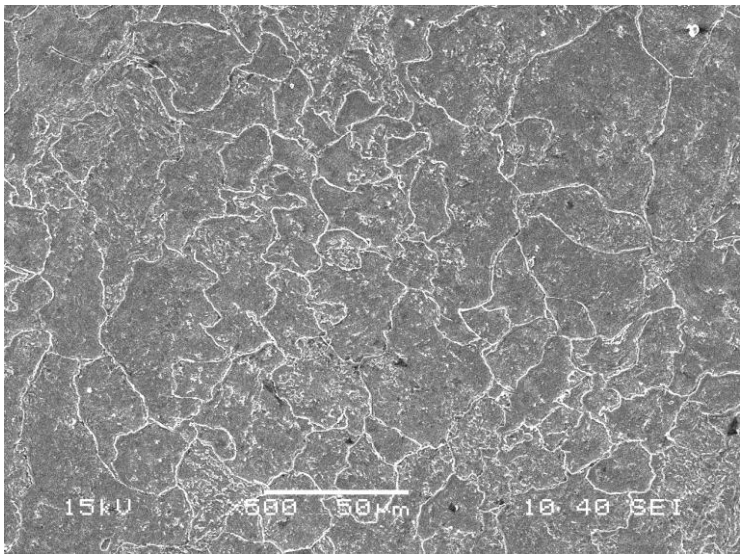

Fig. 4.9: SEM micrograph of Uncoated BH Steel

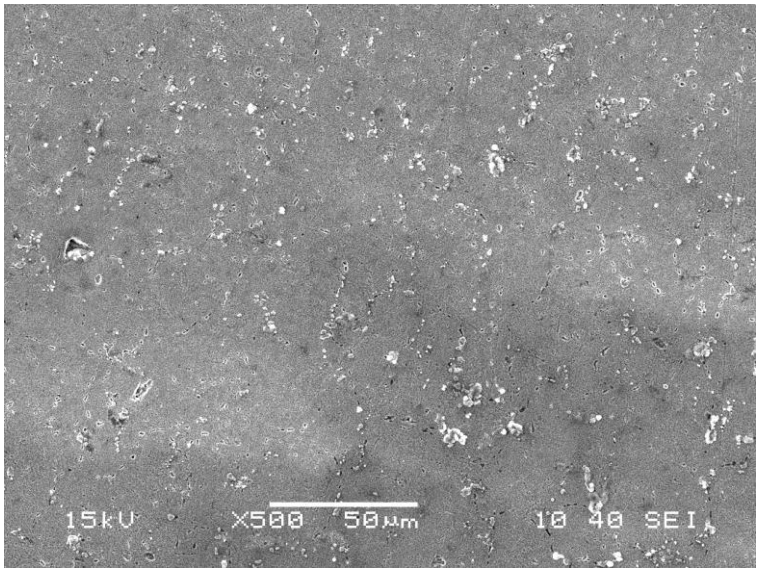

Fig.4.10: SEM micrograph of Uncoated EDD Steel

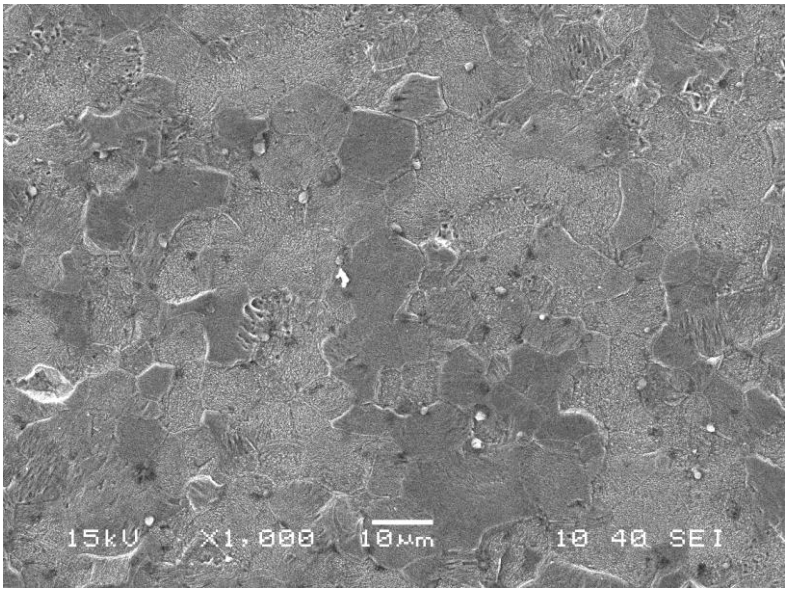

Fig.4.11: SEM micrograph of Uncoated HIF Steel

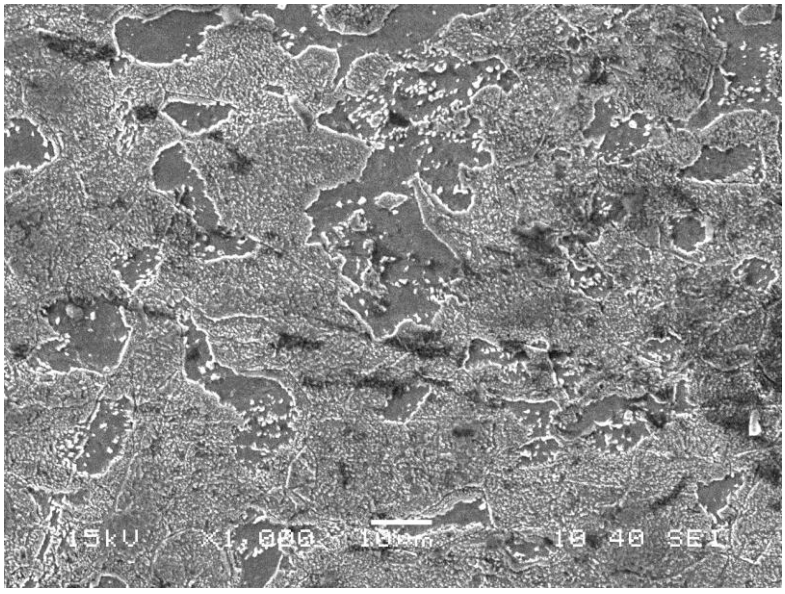

4.12: SEM micrograph Uncoated IF Steel

Fig. 4.13 shows SEM photograph of Cr coated steel. It shows fine nodular structure. The presence of Cr was confirmed by Energy Dispersive Spectroscopy (EDS) as shown in Fig. 4.14. From quantitative analysis 100% Cr was observed.

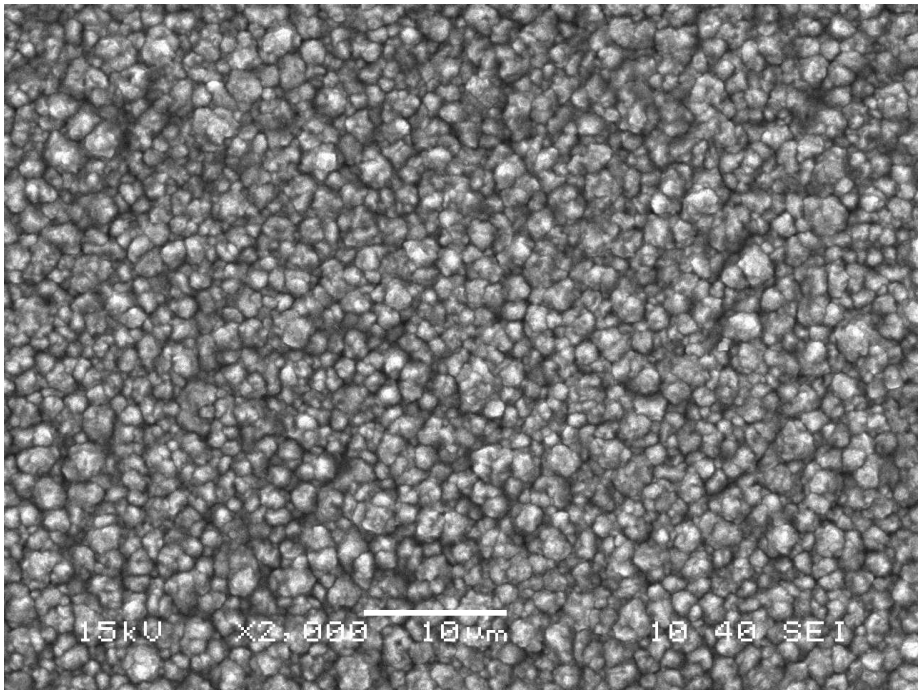

Fig.4.13: SEM micrograph Cr Coated EDD Steel

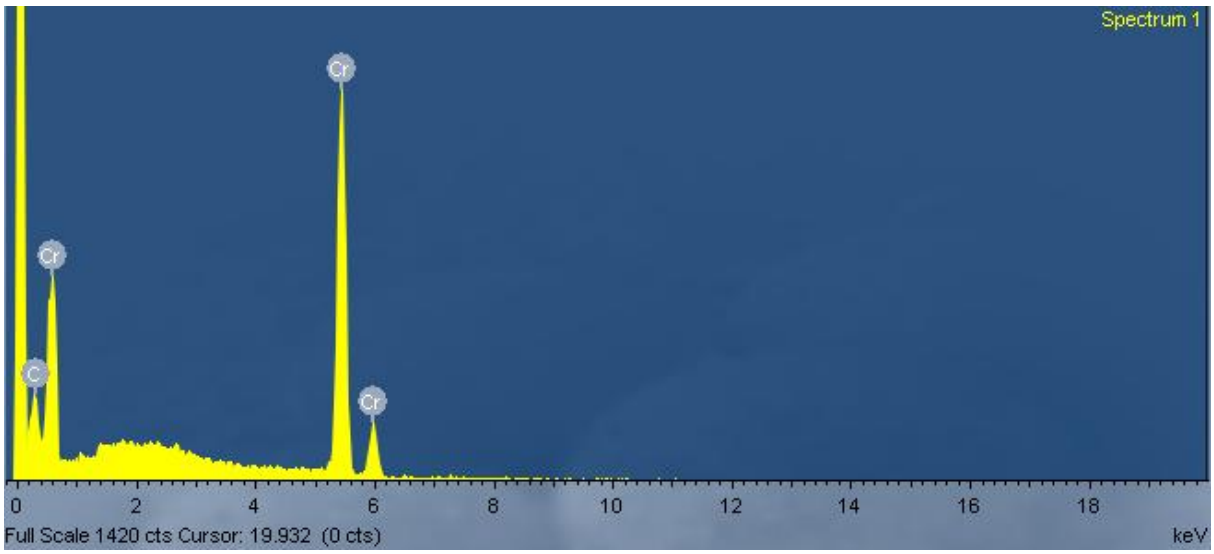

Fig. 4.14: EDS of Cr Coated EDD Steel

Fig. 4.15 shows SEM photograph of Ni coated steel. It shows presence of faceted Nickel structure. The presence of Ni was confirmed by Energy Dispersive Spectroscopy (EDS) as shown in Fig. 4.16. From quantitative analysis 100% Ni was observed.

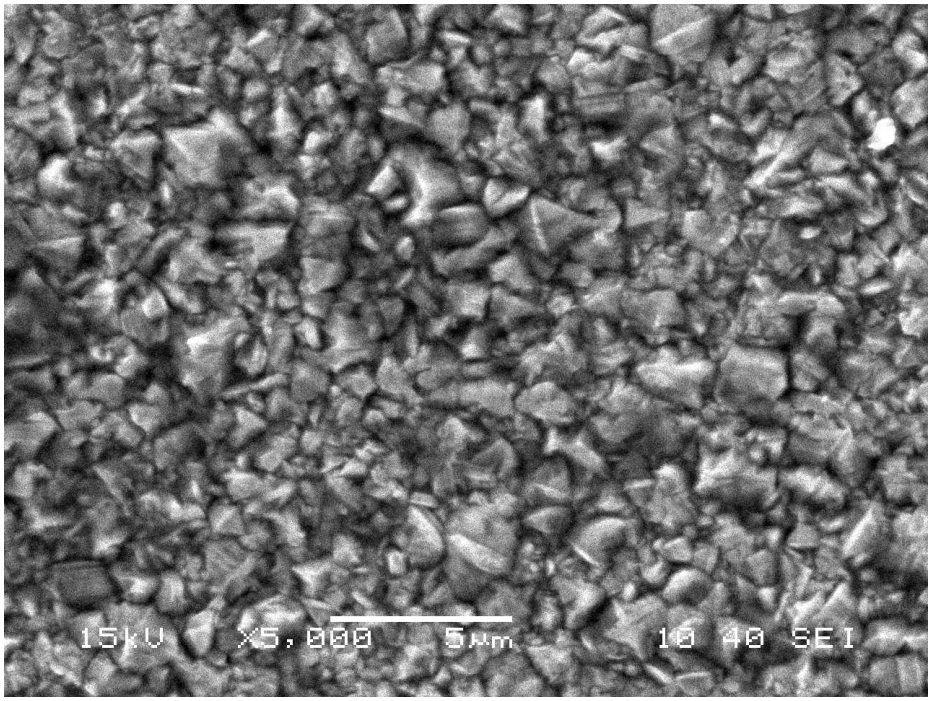

Fig. 4.15: SEM micrograph Ni Coated BH Steel

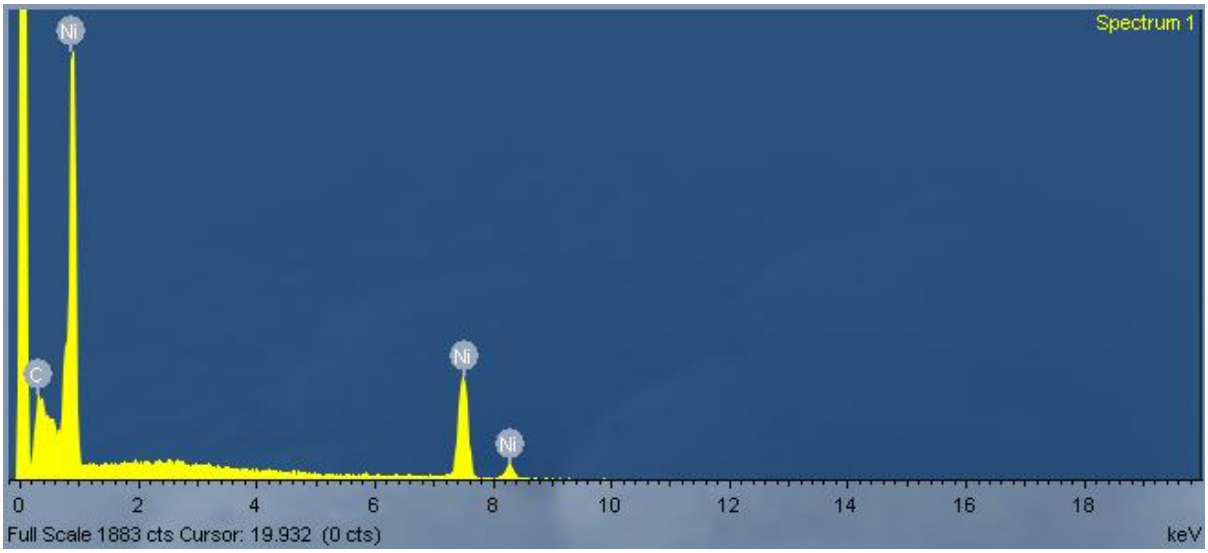

Fig. 4.16: EDS of Ni Coated BH Steel

4.3 Hardness Measurement

To study the surface mechanical properties, microhardness test was carried out on all the coated steel samples. For different substrates no variation on the coating microhardness was observed. Table 4.4 sows the microhardness data, Cr hardness is much higher as compared to the hardness of Ni coating.

Table 4.4: Hardness data of different coatings

Material	Hardness
Cr Coating	980 VHN
Ni Coating	375 VHN

5. Conclusion

I. Nickel and Chromium coating was done successfully on four different steel substrates by electroplating method.

II. Substrate texture study by intensity variation of a particular plane shows different texture in the four substrates.

III. Pole figure study of the substrate does not show wide variation in texture.

IV. Like II and III, coated samples also show variation in intensity of a particular plane but not such variation in pole figure.

V. Little variation in texture of Ni coating of IF steel was observed.

VI. Similar texture result in all the coated samples may be due to the thickness of coating.

VII. Uncoated steels show ferritic microstructure whereas after Ni and Cr coating, only 100% Ni and Cr were observed respectively.

VIII. Microhardness measurement of the coating shows high value of Chromium as compared to Ni coating.

References

1. Materials degradation and its control by surface engineering, Andrew W. Batchelor, Loh Nee Lam, Margam Chandrasekaran, World Scientific Publishing Co. Pte. Ltd., Singapore , 1999
2. Electroplating: Basic Principles, Processes and Practice, Nasser Kanani, Elsevier Science, 2004
3. Surface engineering of metals: principles, equipment, technologies, Tadeusz Burakowski, Tadeusz Wierzchoń, CRC Press , 1998.
4. International Workshop on Surface Engineering and Coatings, Indira Rajagopal, Allied Publishers Ltd., 1999.
5. Elements of X-Ray Diffraction, Cullity B. D, Addision-Wesley Publisher, MA, 1978
6. http://www.eng.utah.edu/~gale/mems/Lecture%2012%20Electrodeposition.pdf
7. ASM Handbook, Volume 5, Surface Engineering ASM International, Materials Park, OH 44073, 1994, page 201
8. Effect of substrate texture on the formation of ξ-phase in the overlying galvannealed coatings in industrially produced interstitial free steels, A. Chakraborty and R.K. Ray, Scripta Mater., 2007, page 653-656.
9. Texture and anisotropy, H R Wenk and P Van Houtte, Reports on Progress in Physics, Volume 67, Number 8, Institute of Physics Publishing,2004
10. Effect of galvannealing power on the texture and powdering resistance of industrially produced galvannealed coating on interstitial free steel, A. Chakraborty, D. Bhattacharjee, R. Pais and R.K. Ray, Scripta Mater., 2007, page 715-718
11. Formability analysis of extra-deep drawing steel, D. Ravi Kumar, Jou. Mater. Process., Technol., 2002, Vol. 130-131,
12. Microstructural and texture studies of gas-nitrided Cr-coated low-alloy high-carbon steel, A. Basu , J. Dutta Majumdar , S. Ghosh Chowdhury , P.K. Ajikumar , P. Shankar , A.K. Tyagi, Surf. Coat. Technol., 2007, page 6985-6992.
13. Shear Rolling and crystallization textures of interstitial free steel sheet, Sang Heon Lee, Dong Nyung Lee, Mater. Sc. Engg. A., 1998, page 84-90.
14. Handbook of mechanical alloy design, George E. Totten, Lin Xie, Kiyoshi Funatani, Marcel Dekker Inc.